

## Effect of superconductivity on near-field radiative heat transfer

Tomáš Králík, Věra Musilová, Tomáš Fořt, and Aleš Srnka

*Institute of Scientific Instruments of the CAS, v. v. i., Královopolská 147, 612 64 Brno, Czech Republic*  
(Received 11 November 2016; revised manuscript received 17 January 2017; published 9 February 2017)

Near-field (NF) radiative heat transfer (RHT) over vacuum space between bodies can exceed the far-field (FF) heat transfer by orders of magnitude. A large portion of the heat flux transferred between metals in NF is at very low frequencies, much lower than in FF. Thus a strong effect of superconductivity on NF RHT can be expected even at radiation temperatures above the superconducting critical temperature, where nearly no effect in FF is observed. We have examined experimentally the RHT between plane-parallel surfaces of niobium. Up to a fivefold decrease in NF heat flux was observed when the colder sample passed from the normal to the superconducting state. We found that a maximum decrease occurs at sample spacings ten times shorter than the spacing of crossover between the NF and FF heat flux, being  $\approx 1000/T$  ( $\mu\text{m}$ ). Applying Polder's and Van Hove's relations for NF RHT and BCS theory of superconductivity, we explain this effect and show the roles of transversal electric and magnetic modes in the steep decrease of heat flux below the critical temperature and the subsequent flux saturation at low temperatures.

DOI: [10.1103/PhysRevB.95.060503](https://doi.org/10.1103/PhysRevB.95.060503)

**Introduction.** Pure metals, owing to their high electrical conductivity, are known to be good reflectors of thermal radiation at infrared and longer wavelengths. The idea that the transition to the superconducting state markedly increases the metal's reflectivity (decreases absorptivity) is justified for far-field (FF) thermal radiation of temperatures below the superconducting critical temperature  $T_c$ . On the other hand, the photons of a thermal source with a temperature higher than  $T_c$  have enough energy to be absorbed by breaking up the Cooper pairs of the superconducting condensate, as follows from the BCS theory of superconductivity [1] and the Planck's characteristic wavelength of FF radiation. This may be markedly different in the near-field regime.

The near field (NF) from a planar source is composed of evanescent waves [2] whose amplitude decays exponentially with the distance from a body's surface. Even though NF is not radiative, another body placed sufficiently near to the surface of a source can absorb a significant amount of the power of the evanescent waves by photon tunneling [3]. In this case, the NF contribution to radiative heat transfer potentially exceeds the Planck's blackbody limit by orders of magnitude [4–6]. A crossover between FF and NF occurs at distances  $d \sim 10^{-1} \lambda$  of the electromagnetic radiation wavelength [7]. In other words, at a given distance  $d$ , the NF spectrum exceeds the spectrum of FF at long wavelengths, which means that NF radiative heat transfer predominately occurs via photons of lower energy than in the FF.

Thus, we assume that thermal NF could open a window for the observation of a strong influence of the superconducting phase transition on radiative heat transfer, even at radiation temperatures, which are higher than the critical temperature  $T_c$ .

NF radiative heat transfer has been studied both theoretically and experimentally for various materials, such as dielectrics [8,9], metals [6,10], graphene [11,12], metamaterials [13], and the  $\text{VO}_2$  undergoing a metal-to-insulator transition [14], to give some examples. For a review, see Refs. [3,13,15]. Studies of the effect of superconductivity on thermal NF heat transfer are lacking. The possibility to extract some information about superconductors when varying the distance between the samples (absorber and

radiator) and their temperatures therefore deserves further investigation. In particular, an interesting question to ask is whether the difference between radiative heat flow in the normal and superconducting states could provide a contrast in the thermal NF microscopy [7,16] of structures made of superconducting materials, or provide some thermal control [14] at low temperatures, with possible applications including thermal switches, diodes, or transistors [17,18], or possibly in microelectromechanical systems [19].

In this Rapid Communication, we present experimental results on NF radiative heat transfer between normal and superconducting metal bodies. We have chosen samples of niobium (Nb) with a plane-parallel vacuum gap between them. The reasons are as follows: (i) With Nb, we can measure over a reasonably large range of temperatures (above a helium bath temperature of 4.2 K) below and above the critical temperature, and (ii) the geometrically simple (although challenging experimentally) plane-parallel configuration enables us to calculate NF heat transfer directly from the relations derived by Polder and Van Hove [4] for infinite plane-parallel surfaces. Let us briefly review some of those relations in question.

**Basic theory.** The total heat flux over the vacuum gap between samples is described by

$$q(T_1, T_2) = \int_0^\infty I(T_1, T_2, \omega) [\mathcal{T}_{\text{TE}}^{\text{FF}} + \mathcal{T}_{\text{TM}}^{\text{FF}} + \mathcal{T}_{\text{TE}}^{\text{NF}} + \mathcal{T}_{\text{TM}}^{\text{NF}}] d\omega. \quad (1)$$

In Eq. (1), the heat flux from the hot to the cold sample, and vice versa, is dependent on the intensities of the blackbody radiation generated within two bodies at temperatures  $T_1$  and  $T_2$ :

$$I(T_1, T_2, \omega) = \frac{1}{\pi} \left( \frac{\omega}{2\pi c} \right)^2 \left[ \frac{\hbar\omega}{\exp(\hbar\omega/k_B T_2) - 1} - \frac{\hbar\omega}{\exp(\hbar\omega/k_B T_1) - 1} \right]. \quad (2)$$

This term is multiplied by the spectral hemispherical transmissivities  $\mathcal{T}$  of the vacuum gap for far-field (superscript FF) and

near-field (NF) radiation of the transversal electric mode (TE) and transversal magnetic mode (TM),

$$T_m^{\text{FF}}(\omega, d) = \int_0^{\omega/c} \frac{1}{2} t_m^{\text{FF}} \frac{2\pi K d K}{(\omega/c)^2}, \quad (3a)$$

$$T_m^{\text{NF}}(\omega, d) = \int_{\omega/c}^{\infty} \frac{1}{2} t_m^{\text{NF}} \frac{2\pi K d K}{(\omega/c)^2}, \quad (3b)$$

where the subscript  $m$  denotes the TE or TM mode of radiation and  $K$  is the surface-parallel component of the wave vector in vacuum,  $K_0 = \omega/c$ .

Spectral directional NF and FF transmissivities of the plane-parallel vacuum gap between samples, integrated in Eqs. (3),

$$t_m^{\text{FF}} = \frac{(1 - |r_m^{(1)}|^2)(1 - |r_m^{(2)}|^2)}{|1 - r_m^{(1)} r_m^{(2)} \exp(2i\gamma_0 d)|^2}, \quad (4a)$$

$$t_m^{\text{NF}} = \frac{4\text{Im}(r_m^{(1)})\text{Im}(r_m^{(2)}) \exp(-2\gamma''_0 d)}{|1 - r_m^{(1)} r_m^{(2)} \exp(-2\gamma''_0 d)|^2}, \quad m = \text{TE, TM}, \quad (4b)$$

are given by the Fresnel reflection coefficients  $r$  of the sample surface, distinguished by the superscript. Notice that in the exponential terms in Eqs. (4) (i.e., the “interference term” in FF, and the decaying term in NF), the real values  $\gamma_0 = [(\omega/c)^2 - K^2]^{1/2}$  ( $K < K_0 = \omega/c$ ) and  $\gamma''_0 = [K^2 - (\omega/c)^2]^{1/2}$  ( $K > K_0$ ) are multiplied by the distance  $d$  between the surfaces. For the effect discussed in this Rapid Communication, Eq. (4b) is substantial, where the imaginary part of the Fresnel coefficients is crucial for the strength of the NF and the decaying exponential term suppresses short wavelengths.

To calculate the Fresnel coefficients in Eqs. (4), we used the computer code published in Ref. [20] for the evaluation of the dynamic electrical conductivity of a superconductor. This code, based on the Mattis and Bardeen theory [21], takes into account the arbitrary purity of the superconductor. In the normal state, the conductivity coincides with the Drude model,

$$\sigma(\omega) = \sigma_1(\omega) + i\sigma_2(\omega) = \frac{\sigma_{\text{dc}}}{1 - i\omega\tau}, \quad (5)$$

$$\sigma_{\text{dc}} = \varepsilon_0 \omega_p^2 \tau,$$

where  $\sigma_{\text{dc}}, \varepsilon_0, \omega_p$ , and  $\tau$  stand for the dc conductivity measured in the normal state, the vacuum permeability, the plasma frequency, and the relaxation time of free electrons, respectively. As input parameters for the theoretical model, we have applied the measured values of dc conductivity  $\sigma_{\text{dc}} = 1.7 \times 10^7 \text{ S}$  and critical temperature  $T_c = 8.995 \text{ K}$  on one hand, and the literature values of the plasma frequency of niobium  $\omega_p = 8.8 \times 10^{15}$  [22] and the relation for the energy gap at  $T = 0 \text{ K}$ ,  $E_{g0} = 3.528 kT_c$  [1] on the other hand. Values of the energy gap  $E_{gT}$  at temperatures  $0 < T < T_c$  were obtained by interpolation from the table of reduced energy gap  $E_{gT}/E_{g0}$  vs  $T/T_c$  provided in Ref. [23].

*Experimental setup.* Both the radiator and absorber samples are 548 nm thick Nb layers deposited by dc magnetron sputtering on circular sapphire substrates 35 mm in diameter and 2.7 mm in thickness with a planarity of better than 0.5  $\mu\text{m}$ , appearing optically smooth. The reverse side and

sidewalls of the sample substrates have extra Al and Cu thin layers. The Al layer suppresses the absorption or emission of parasitic background radiation while the Cu “patches” serve as contact electrodes for *in situ* capacitive measurements of the vacuum gap size  $d$  between the sample surfaces, which are in a concentric plane-parallel position.

Four-point probe measurements of dc resistivity of the samples resulted in a room-temperature value, which is 1.38 times higher than the one published for the bulk Nb [24] and a low-temperature resistivity of about  $5.9 \times 10^{-8} \Omega \text{ m}$ , which is nearly constant at temperatures from 9 to 30 K (room-temperature resistivity to residual resistivity ratio, RRR = 3.6). On decreasing the temperature further, we observed a transition to the superconducting state at a critical temperature of  $(8.995 \pm 0.020) \text{ K}$ , seen as a steep decrease within an interval of about 10 mK (inset in Fig. 2). The four-point probe measurement was conducted on the samples just before their installation into the dedicated Evanescent Wave Apparatus (EWA) [25], designed by us for previous NF heat transfer measurements [6]. The EWA has been updated for the current experiment with an additional stabilized heater for setting various temperatures  $T_1$  of the cooler sample with a stability of better than 50  $\mu\text{K}$ . Sample spacing  $d$  is set *in situ* with a differential micrometric screw and its value can be read out in parallel with an independent capacitive measurement of the spacing, ranging from hundreds down to a few micrometers. An uncertainty of less than 1.5  $\mu\text{m}$  in the distance  $d$  was assessed from a comparison between the readouts on the screw and the capacitometer.

*Results.* Figure 1 collects all experimental data. We measured the heat flux  $q$  between the Nb film in the normal state (radiator) at the temperature  $T_2 = 12.5, 15, 20,$  and  $30 \text{ K}$  and the film passing from the normal to superconducting state (absorber) at  $T_1 = 5\text{--}9.9 \text{ K}$  for various values of spacing between the samples,  $d = 7.5\text{--}600 \mu\text{m}$ . The heat flux  $q$  transferred between the samples is normalized to the FF heat flux between the black (100% absorbing) surfaces,

$$q_{\text{BB}} = \sigma_{\text{SB}}(T_2^4 - T_1^4), \quad (6)$$

where  $\sigma_{\text{SB}}$  is the Stefan-Boltzmann constant. The values of the normalized heat flux  $q/q_{\text{BB}}$  are plotted depending on the product of the temperature  $T_2$  of the radiator and vacuum gap size  $d$ . Normalized heat flux measured for various temperatures  $T_2$  of the radiator and spacing  $d$  at the constant absorber temperature  $T_1 = 9.1 \text{ K}$  (normal state) tend to follow one dependence on  $T_2 d$  at short distances. A similar tendency is seen in the data points measured with the absorber in the superconducting state at  $T_1 = 5 \text{ K}$ . This behavior is, under certain conditions, related to the exponential terms in Eqs. (2) and (4b).

From now on, for brevity, we will use the term “contrast”  $C$ , defined at a specific value of product  $T_2 d$  as the ratio between the data for the absorber in the normal state at  $T_1 = 9.1 \text{ K}$  and the superconducting state at  $T_1 = 5 \text{ K}$ :

$$C(T_2, d) = q(9.1 \text{ K}, T_2, d)/q(5 \text{ K}, T_2, d). \quad (7)$$

We have plotted the contrast  $C$  in the upper inset of Fig. 1. The theoretical curve gives a higher contrast than the measured values and shows a maximum at about  $T_2 d = 70 \text{ K } \mu\text{m}$ . A decrease of contrast at low values of  $T_2 d$  can be expected since

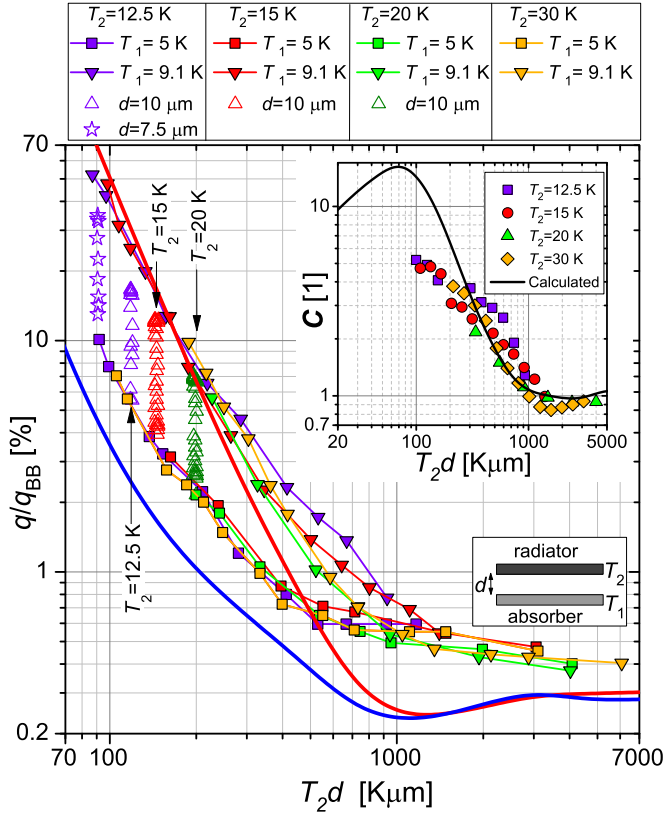


FIG. 1. Main panel: Heat flux  $q/q_{\text{BB}}$  [normalized to blackbody, Eq. (6)], dependence on the product of the temperature  $T_2$  of the “hot” surface (radiator) and spacing  $d$  between the radiator and the “cold” surface (absorber). Solid symbols show data measured when the spacing  $d$  was varied at a specific temperature  $T_2$ , whereas the absorber was at  $T_1 = 5$  K (superconducting) or 9.1 K (normal state). The open symbols are points measured for various absorber temperatures  $T_1$  at specific values of  $d$  (data are plotted in Fig. 2 as a function of  $T_1$ ). Theoretical curves (thick solid lines) evaluated for  $T_1 = 5$  and 9.1 K, both for  $T_2 = 15$  K. Upper inset: Contrast  $C$ , Eq. (7). The theoretical line is calculated for  $T_2 = 15$  K. Lower inset: Scheme of the sample configuration.

shorter and shorter wavelengths are involved with decreasing the spacing and thus the spectrum of the transferred NF photons shifts toward higher energies above the energy gap.

Data visualized with open symbols in Fig. 1 were obtained at specific distances  $d$  and radiator temperatures  $T_2 (> T_c)$ . Both were kept constant during each run, when we varied the absorber temperature  $T_1$  between 5 and 9.9 K step by step, crossing the superconducting critical temperature. These open symbol data are replotted in Fig. 2 as a function of the absorber temperature  $T_1$ .

In Fig. 2, we see that at  $T_1^* = (8.97 \pm 0.02)$  K, the NF regime is characterized by a steep decrease in heat transfer before saturating below  $T_1 \sim 8.5$  K. The value  $T_1^*$  agrees with the critical temperature of the transition to the superconducting phase,  $T_c = (8.995 \pm 0.020)$  K (cf. the inset in Fig. 2).

*Discussion.* Figure 3 shows the heat fluxes evaluated using Eq. (1) together with the experimental data for  $d = 10 \mu\text{m}$  and  $T_2 = 15$  K. The theoretical curves, essentially following the behavior of the experimental data, clearly show that the

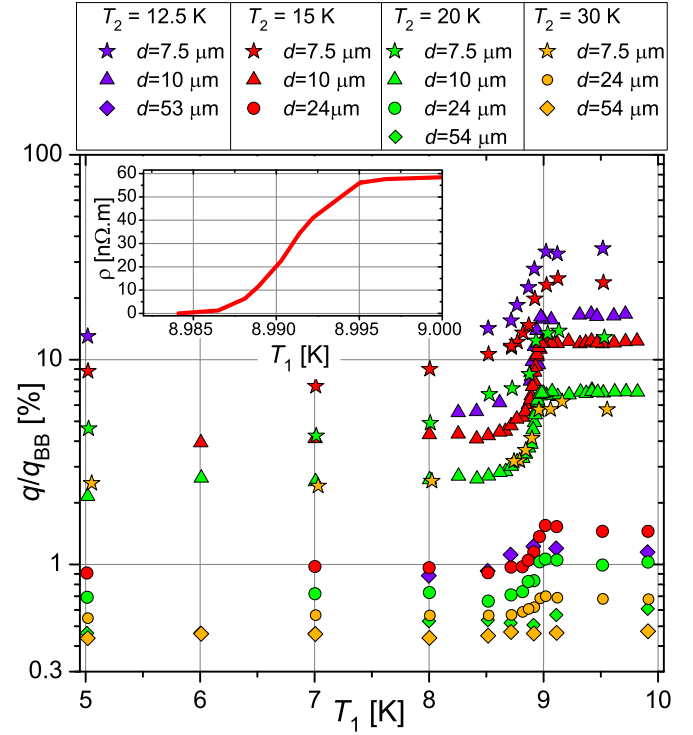


FIG. 2. Main panel: Heat flux  $q/q_{\text{BB}}$  as a function of the absorber’s temperature  $T_1$ . Data are plotted for various values of spacing  $d$  and radiator temperature  $T_2$  within the interval  $T_2 d = 90 - 4000$  K  $\mu\text{m}$ . The phase transition from a normal metal to a superconductor manifests itself as a steep decrease in heat transfer at  $T_1 < T^* = (8.97 \pm 0.02)$  K. Inset: Temperature dependence of electrical dc conductivity of the Nb layer. The critical temperature  $T_c = (8.995 \pm 0.020)$  K and the steep transition to superconductivity within an interval of 10 mK are visible.

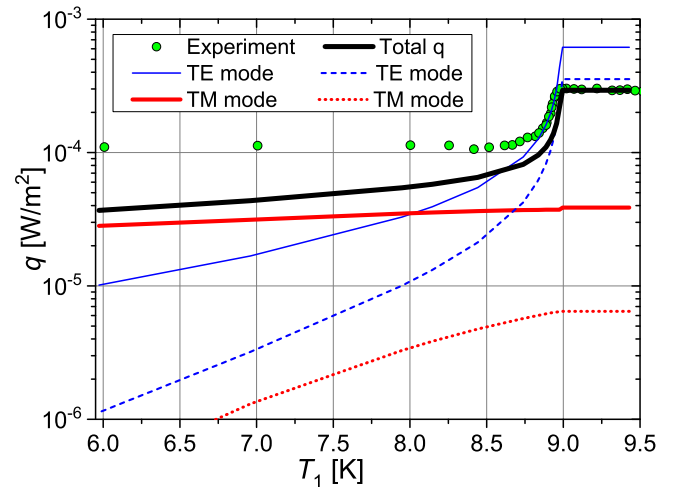


FIG. 3. Near-field heat flux  $q$  transferred between Nb layers separated by  $d = 10 \mu\text{m}$  (circles). The absorber at temperature  $T_1$  undergoes a phase transition to the superconducting state at  $T = 8.995$  K. The radiator is in the normal state at  $T_2 = 15$  K. Contributions of the near-field TE and TM modes are calculated separately using Eq. (1). Far-field heat flux is negligible in this case. Heat fluxes from the radiator at  $T_2$  to the absorber at  $T_1$  (solid lines) and vice versa (dashed lines) are distinguished. The difference between them gives the total heat flux (thick line).

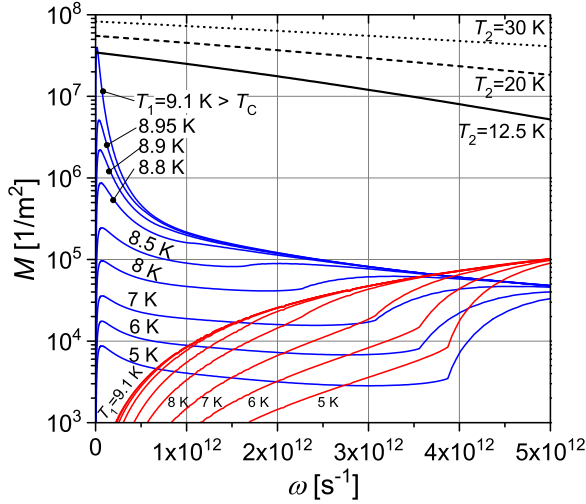


FIG. 4. Modified NF transmissivities  $M$  of near-field TE radiation mode (curves with peaks at low frequency  $\omega$ , blue line) and TM mode (curves increasing monotonically with frequency, red lines), calculated at  $d = 10 \mu\text{m}$ , Eq. (8a). Kinks on the curves correspond to the superconducting energy gap of the absorber at individual temperatures  $T_1$ . Upper curves (black lines) present the term  $\bar{E}$  in Eq. (8b) multiplied by a constant.

steep decrease below the critical temperature is due to the TE mode, while the TM mode is responsible for the saturation. This behavior is due to the dominant NF of the TE mode at low frequencies, while at high frequencies the TM mode dominates [10]. To show it in our experiment, we neglect the heat flux from the absorber to the radiator, the second term in Eq. (2), and separate the NF terms of the integrand in Eq. (1) into two parts:

$$M_m \equiv \frac{1}{\pi} \left( \frac{\omega}{2\pi c} \right)^2 T_m^{\text{NF}}(T_1, T_2, \omega, d), \quad m = \text{TE, TM}, \quad (8a)$$

$$\bar{E} \equiv \frac{\hbar\omega}{\exp(\hbar\omega/k_B T_2) - 1}, \quad (8b)$$

$$q(T_1, T_2) \approx \int_0^\infty \bar{E}(T_2, \omega) M_m(T_1, \omega, d) d\omega. \quad (8c)$$

The term  $M$ , further called the “modified NF transmissivity” of the vacuum gap, does not depend on the temperature  $T_2$  at all in our experiment (the conductivity of our Nb sample, and consequently the transmissivities, do not vary with the temperature  $T_2$  from 9 to 30 K).

In Fig. 4 we plot the modified transmissivity  $M$  calculated for various temperatures  $T_1$  at a fixed spacing  $d = 10 \mu\text{m}$ . At absorber temperatures  $T_1 > 8.5 \text{ K}$ , the TE mode transmissivity shows a high peak, followed by a monotonic decrease with frequency. This shows that the TE mode contributes significantly to the total heat flux at low frequencies, far below the energy gap (for heat flux spectra, see Ref. [26]). Immediately after the superconducting transition, the real part of the dielectric function dramatically increases in an absolute value at low frequencies, which is accompanied by a decrease in the imaginary part of the Fresnel coefficients [26]. As a result, in the superconducting state, the low-frequency TE

mode transmissivity  $M$  is strongly suppressed with decreasing temperature  $T_1$  and, correspondingly, the heat flux steeply decreases. On the other hand, even though the modified TM transmissivities  $M$  are affected by superconductivity, their low values at low frequencies are followed by a monotonic increase with frequency, exceeding the values of the TE mode at high frequencies. Thus, the spectrum of the energy transferred by the TM mode is primarily above the energy gap and thus the TM mode flux is weakly affected by the superconducting state.

The differences between the measured and theoretical data may be due (in part) to experimental difficulties, such as distortion of the plane parallelism. Nevertheless, this cannot explain the theoretical contrast being markedly higher than the measured one. We expect that better quantitative agreement can be achieved either by a refined theory, taking into account the structure defects in sputtered Nb films [22,27,28], typically characterized by low RRR, or by trying to manufacture Nb films with higher RRR. Our goal here was to prove experimentally the effect of the energy gap of the superconducting state on radiative heat transfer in the NF regime. Nevertheless, BCS theory, suitable for the interpretation of dynamical conductivity in bulk Nb [29] with high RRR, well describes the observed effect qualitatively.

*Conclusion.* We studied experimentally the radiative heat transfer between plane-parallel niobium samples during the phase transition of the colder sample (absorber) from the normal to the superconducting state ( $T_c = 9.0 \text{ K}$ ) and interpreted it in terms of the BCS theory. The temperature of the hot sample (radiator) was varied between 12.5 and 30 K. In the NF regime, we observed a substantial heat flux decrease at the transition to the superconducting state [contrast, Eq. (7), between the normal and superconducting state up to a factor of 5] differing dramatically from the situation in FF heat transfer, where no effect of superconductivity was observed. A steep decrease of the NF heat flux sets in at the critical temperature of Nb and is saturated below an absorber temperature of about 8.5 K. Theoretical dependencies, semiquantitatively agreeing with the experimental ones, show the following: (i) A marked contrast between NF heat transfer with the absorber in the normal and in the superconducting state can be achieved at radiator temperatures several times higher than the superconducting critical temperature. (ii) A maximum in the contrast is expected at distances about ten times shorter than the distance of the crossover between FF and NF heat transfer. (iii) The steep decrease of heat flux below the critical temperature is caused by the low-frequency contribution of the TE polarization mode (far below the energy gap  $\omega_g \equiv E_g/\hbar$  of the superconducting state), which dominates the NF heat transfer of pure metals and which is strongly suppressed by absorber superconductivity. (iv) The saturation of the NF heat flux at low temperatures is caused by the TM mode, which, due to its weak NF effect, contributes (similarly to FF) at higher frequencies and is thus weakly sensitive to absorber superconductivity.

It would be useful to examine more generally the properties of the effect observed here for Nb samples using calculations and experiment with another BCS superconductor, such as NbN, for example. Based on our BCS calculations and experiment, we expect an optimum value of RRR (higher than our value 3.6) where the effect will be more pronounced.

We thank D. Munzar and M. Macek for valuable discussions and support, P. Hanzelka for advice on experimental improvements, M. Zobač and M. Kasal for the design of the electronic system for capacitance measurement, and we acknowledge

support by the Czech Science Foundation (GA CR) under Grant No. GA14-07397S and by Ministry of Education, Youth and Sports (MEYS) of the Czech Republic (Project No. LO1212).

- 
- [1] M. Tinkham, *Introduction to Superconductivity*, 2nd ed. (McGraw-Hill, New York, 1996).
- [2] M. Born and E. Wolf, *Principles of Optics* (Cambridge University Press, Cambridge, U.K., 1999).
- [3] S. Basu, *Near-Field Radiative Heat Transfer Across Nanometer Vacuum Gaps* (Elsevier, Amsterdam, 2016).
- [4] D. Polder and M. Van Hove, *Phys. Rev. B* **4**, 3303 (1971).
- [5] A. Kittel, W. Muller-Hirsch, J. Parisi, S. A. Biehs, D. Reddig, and M. Holthaus, *Phys. Rev. Lett.* **95**, 224301 (2005).
- [6] T. Kralik, P. Hanzelka, M. Zobač, V. Musilova, T. Fort, and M. Horak, *Phys. Rev. Lett.* **109**, 224302 (2012).
- [7] J. B. Pendry, *J. Phys.: Condens. Matter* **11**, 6621 (1999).
- [8] K. Joulain, J. P. Mulet, F. Marquier, R. Carminati, and J. J. Greffet, *Surf. Sci. Rep.* **57**, 59 (2005).
- [9] J. J. Greffet, R. Carminati, K. Joulain, J. P. Mulet, S. P. Mainguy, and Y. Chen, *Nature (London)* **416**, 61 (2002).
- [10] P. O. Chapuis, S. Volz, C. Henkel, K. Joulain, and J. J. Greffet, *Phys. Rev. B* **77**, 035431 (2008).
- [11] V. B. Svetovoy, P. J. van Zwol, and J. Chevrier, *Phys. Rev. B* **85**, 155418 (2012).
- [12] P. J. van Zwol, S. Thiele, C. Berger, W. A. de Heer, and J. Chevrier, *Phys. Rev. Lett.* **109**, 264301 (2012).
- [13] X. Liu, L. Wang, and Z. M. Zhang, *Nanoscale Microscale Thermophys. Eng.* **19**, 98 (2015).
- [14] P. J. van Zwol, L. Ranno, and J. Chevrier, *Phys. Rev. Lett.* **108**, 234301 (2012).
- [15] B. Song, A. Fiorino, E. Meyhofer, and P. Reddy, *AIP Adv.* **5**, 053503 (2015).
- [16] A. Kittel, U. F. Wischnath, J. Welker, O. Huth, F. Rüting, and S.-A. Biehs, *Appl. Phys. Lett.* **93**, 193109 (2008).
- [17] W. Gu, G. H. Tang, and W. Q. Tao, *Int. J. Heat Mass Transfer* **82**, 429 (2015).
- [18] P. Ben-Abdallah and S.-A. Biehs, *Phys. Rev. Lett.* **112**, 044301 (2014).
- [19] R. St-Gelais, L. X. Zhu, S. H. Fan, and M. Lipson, *Nat. Nanotechnol.* **11**, 515 (2016).
- [20] W. Zimmermann, E. H. Brandt, M. Bauer, E. Seider, and L. Genzel, *Physica C* **183**, 99 (1991).
- [21] D. C. Mattis and J. Bardeen, *Phys. Rev.* **111**, 412 (1958).
- [22] A. V. Pronin, M. Dressel, A. Pimenov, A. Loidl, I. V. Roshchin, and L. H. Greene, *Phys. Rev. B* **57**, 14416 (1998).
- [23] B. Muhlschlegel, *Z. Phys.* **155**, 313 (1959).
- [24] D. R. Lide, *CRC Handbook of Chemistry and Physics: A Ready-Reference Book of Chemical and Physical Data*, 73rd ed. (CRC Press, Boca Raton, FL, 1992).
- [25] T. Kralik, P. Hanzelka, V. Musilova, A. Srnka, and M. Zobač, *Rev. Sci. Instrum.* **82**, 055106 (2011).
- [26] See Supplemental Material at <http://link.aps.org/supplemental/10.1103/PhysRevB.95.060503> for optical constants of studied Nb, Fresnel coefficients, and spectra of transferred energy.
- [27] A. Andreone, A. Cassinese, M. Iavarone, R. Vaglio, I. I. Kulik, and V. Palmieri, *Phys. Rev. B* **52**, 4473 (1995).
- [28] J. Halbritter, *Phys. Rev. B* **60**, 12505 (1999).
- [29] O. Klein, E. J. Nicol, K. Holczer, and G. Gruner, *Phys. Rev. B* **50**, 6307 (1994).